COMMUNICATION

Efficient Triplet Exciton Fusion in Molecularly Doped Polymer Light-Emitting Diodes

*Dawei Di, Le Yang, Johannes M. Richter, Lorenzo Meraldi, Rashid M. Altamimi, Ahmed Y. Alyamani, Dan Credgington, Kevin P. Musselman, Judith L. MacManus-Driscoll, and Richard H. Friend**

When an organic light-emitting diode (OLED) is in operation, 75% of electron–hole recombination events are in spin-triplet configurations and only 25% are in spin-singlet configuration. In conventional fluorescent OLEDs,[1,2] the generation of photons is achieved from the radiative recombination of singlets. Relaxation of triplet excitons is quantum mechanically forbidden. Phosphorescent OLEDs overcome this restriction by allowing the triplet excitons to radiatively decay to the ground state.[3,4] This effect was achieved using strong spin–orbit coupling due to the presence of heavy metal elements in the molecular emitters. More recently, highly efficient OLEDs based on thermally activated delayed fluorescence (TADF) molecules were realized. In TADF emitters, triplet-to-singlet upconversion at room temperature is possible due to a small singlet–triplet energy gap.[5] Another strategy to utilize triplet excitons in fluorescent OLEDs is through the generation of singlets by triplet–triplet annihilation (TTA) or "triplet fusion."[6–8] At the same time, photon upconversion through TTA has been widely considered for next-generation photovoltaic applications.[9–14] Effective upconverters have been demonstrated using combinations of a triplet sensitizer such as platinum octaethylporphyrin (PtOEP)[3] and a triplet acceptor/annihilator such as 9,10-diphenylanthracene (DPA),[15] perylene,[16] or rubrene.[17] TTA-upconversion (TTA-UC) quantum yield (ratio of upconverted photons to absorbed photons) of 30% was observed in solution phase.[18] This suggests that the intrinsic efficiency of the TTA-UC reaction (i.e., the probability of a triplet pair forming a singlet) in solution is >60%, much higher than the spin-statistical prediction of 25% (one pair of triplets collides to form one of the four states: one singlet S_1 and three triplets T_1, assuming higher triplet and quintet states are inaccessible). Practical application of solar energy conversion requires the TTA-UC material to be in solid state rather than in solution phase. However, the TTA-UC quantum yield of solid-state systems remains low, typically below 5%,[10] and is moderately high (about 10%) in only one example.[19] To achieve high efficiencies, high excitation intensities (200 mW cm^{-2} or above) are commonly required. These imply that in solid state, the experimentally observed reaction efficiency of TTA-UC was up to about 20%, below the 25% spin-statistical limit.

To achieve highly efficient triplet fusion (TTA-UC) in OLEDs and other TTA upconverters, we consider four criteria for the selection of emitters: (1) high fluorescence quantum yield, (2) short singlet lifetime, (3) long triplet lifetime, and (4) the energy of two triplet excitons, $2E(T_1)$ lies slightly above that of the singlet exciton, $E(S_1)$, but below the second triplet state, $E(T_2)$ (and also the energies of any spin-quintet states) ($E(S_1) \lesssim 2E(T_1) < E(T_2)$). The first and second criteria are prerequisites for efficient fluorescence. The third criterion is essential for the accumulation of a sufficiently high triplet population density required for rapid triplet–triplet collision processes. The fourth criterion ensures that higher-lying triplet or quintet states do not provide loss channels. The spin states of the triplet excitons give in principle nine spin configurations for the interacting triplet exciton pair, five associated with a quintet, three with a triplet, and one with the singlet state. It is generally considered that the quintet is always higher in energy than the initial triplet pair, so is neglected. If there are no energetically accessible higher-lying triplet states at $E(T_2)$, we expect only the S_1 and T_1 excitons to form. Triplets produced from this reaction can be recycled and participate in a further fusion reaction.[7]

The basic working principle of a triplet fusion LED (FuLED) is illustrated in **Figure 1**a. The initial stage (Stage I) of the device operation includes charge injection and exciton formation. Exciton formation on the emissive molecules may occur directly or indirectly through an additional exciton transfer step from a host material. If a host material is present, the S_1 and T_1 of the host are required to be higher than that of the emitter to allow efficient host-emitter energy transfer and to ensure long triplet lifetime of the emitter (Criterion 3 discussed above). The 25% singlet population can be converted to light emission (and nonradiative losses) from the singlet channel immediately, resulting in prompt electroluminescence (EL). The 75% triplet excitons remain nonemissive, but the population of triplets is

Dr. D. Di, L. Yang, J. M. Richter, L. Meraldi,
Dr. D. Credgington, Prof. R. H. Friend
Cavendish Laboratory
University of Cambridge
JJ Thomson Avenue, Cambridge CB3 0HE, UK
E-mail: rhf10@cam.ac.uk
Dr. R. M. Altamimi, Dr. A. Y. Alyamani
King Abudulaziz City for Science and Technology
Riyadh 12371, Saudi Arabia
Prof. K. P. Musselman
Mechanical and Mechatronics Engineering
University of Waterloo
200 University Avenue West, Waterloo, Ontario N2L 3G1, Canada
Prof. J. L. MacManus-Driscoll
Department of Materials Science and Metallurgy
University of Cambridge
Cambridge CB3 0FS, UK

DOI: 10.1002/adma.201605987

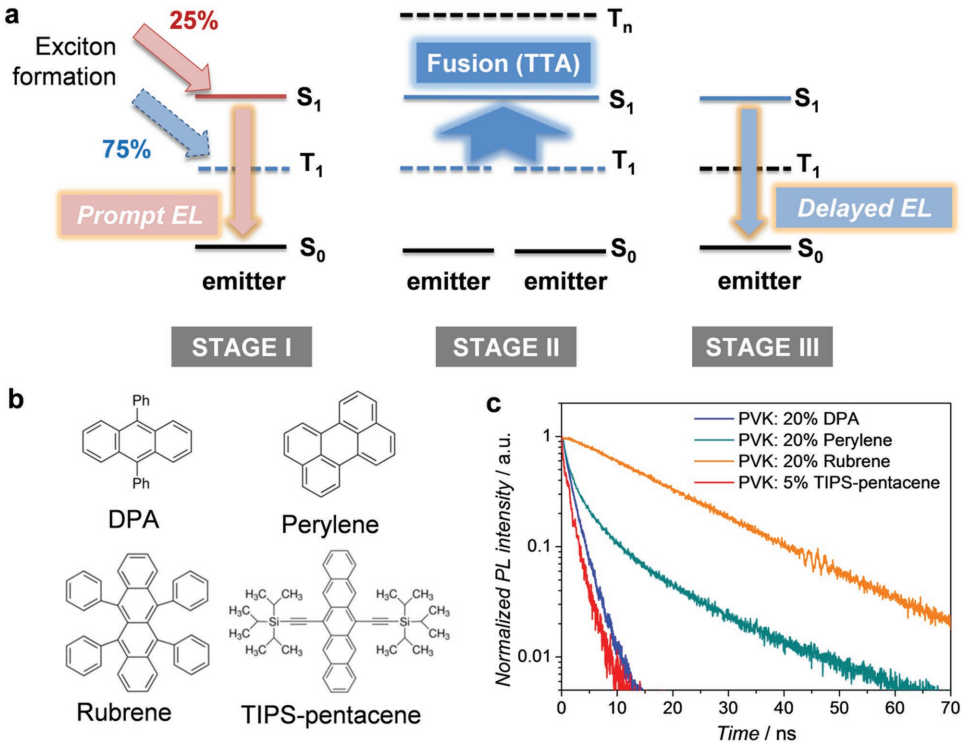

Figure 1. Working principle and materials. a) Working principle of a FuLED. b) Molecular structures of TTA-UC (triplet fusion) emitters. c) PL decay kinetics of the TTA-UC emitters in a wide bandgap polymer host (PVK).

being built up during the process. In Stage II, triplet excitons from a pair of emitter molecules encounter each other and they collide to form a singlet. This reaction obeys spin conservation and is referred to as triplet fusion or TTA-UC in the upconversion literature.[9–14] In Stage III, the triplet-fusion-generated singlet recombines and produces delayed emission.

We recast the triplet-recycling process described in Ref. [7] The ratio of singlet excitons generated by the triplet fusion reaction versus the total exciton population before the reaction can be characterized *by* f_{fusion} and is given by the following:

$$f_{fusion} = f_s\frac{(1-f_s)}{2} + f_s\left[\frac{(1-f_s)}{2}\right]^2 + f_s\left[\frac{(1-f_s)}{2}\right]^3 + \ldots + f_s\left[\frac{(1-f_s)}{2}\right]^n = f_s \times \sum_{n=1}^{n=\infty}\left(\frac{1-f_s}{2}\right)^n = f_s\frac{1-f_s}{1+f_s} \quad (1)$$

where f_s is the probability of singlet generation for each reaction. Assuming f_s = 25% based on spin statistics, we obtain f_{fusion} = 15%. It predicts that, in the case where triplets are formed and recycled during the TTA process, the fraction of delayed fluorescence in EL is $f_{delayed}$ = 15%/(15% + 25%) = 37.5%. And the highest internal quantum efficiency (IQE) of the OLED device can be revised to $IQE_{theoretical}$ = 15% + 25% = 40%.

An alternative and more preferred scenario of TTA-UC in FuLEDs or TTA upconverters is that the TTA process generates singlets only. In this case, f_{fusion} is given by:

$$f_{fusion} = \frac{1-f_s}{2} \quad (2)$$

which gives f_{fusion} = 37.5% by assuming f_s = 25%. It predicts that the maximum fraction of delayed EL from TTA is $f_{delayed}$ = 37.5%/(37.5% + 25%) = 60%, and the highest IQE of the OLED device is $IQE_{theoretical}$ = 37.5% + 25% = 62.5%, higher than that of the triplet-recycling case discussed previously.

In this work, we design and demonstrate molecularly doped polymer FuLEDs. We use simple organic fluorophors including DPA,[15] perylene,[16] and rubrene,[17] which were used in photon upconverters for photovoltaics, and a solution-processable singlet-fission sensitizer, 6,13-bis(triisopropylsilylethynyl) pentacene (TIPS-pentacene),[20,21] as the emissive dopants for FuLEDs. The molecular structures of these emitters are shown in Figure 1b. Apart from the TTA-upconversion molecules, we consider TIPS-pentacene as a potential candidate for triplet fusion, since its deep-lying T_1 state fulfills $E(S_1) \sim 2E(T_1)$ (Criterion 4). This work represents the first application of DPA, perylene, and TIPS-pentacene as OLED emitters.

Using solution processing, we doped each kind of emissive molecules into poly(9-vinylcarbazole) (PVK),[4,22] a wide-bandgap polymer host matrix for OLEDs. The photoluminescence (PL) spectra of the PVK:dopant blends show emission primarily from the dopant molecules under laser excitation (Figure S1, Supporting Information). The PL decay kinetics of the emission peak for each molecule/PVK blend is recorded using time-correlated single photon counting (TCSPC) (Figure 1c). The PL decay processes of all emitters are of singlet character, as expected from fluorescent molecules. The fluorescence lifetimes of DPA, rubrene, and TIPS-pentacene are 1.8, 17.5, and 1.4 ns, respectively. We note that the PL of perylene originates from an exciplex state,[23] with biexponential decay lifetimes of 1.5 and 10.7 ns.

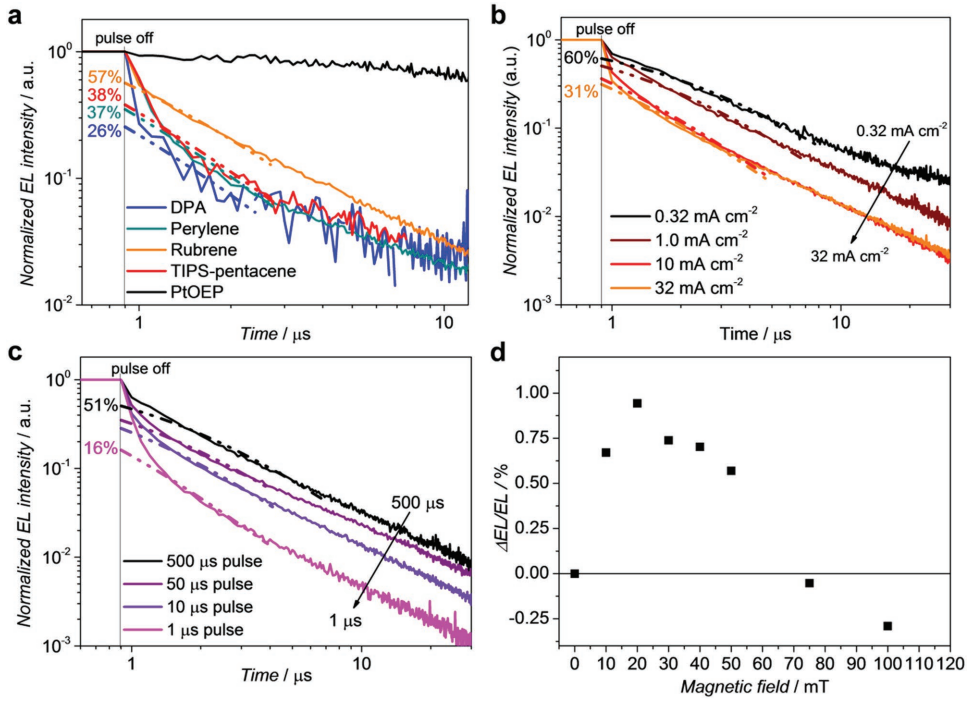

Figure 2. Transient-EL and magneto-EL measurements. a) Transient-EL of various emitters after holding the devices at a current density of 1 mA cm^{-2}. Dashed lines are fits to Equation (3). b) Transient-EL of the rubrene device at different current densities. c) Transient-EL of the rubrene device under different current pulse widths at a current density of 1 mA cm^{-2}. d) Magneto-EL of the device under low-field (B < 100 mT) condition.

To examine whether triplet excitons in these emitters contribute to the EL process, we performed transient-EL measurements for FuLEDs based on PVK:emitter blends. The EL decay profiles for various emitters are shown in **Figure 2**a. The EL of the four fluorophors has an instrumentally limited fast (prompt) decay due to direct recombination of singlets. Investigating detailed kinetics of the prompt fluorescence is beyond the scope of this work. Importantly, it can be seen that the delayed EL component follows a bimolecular decay function:[7]

$$\mathrm{EL}_{\mathrm{delayed}} = \frac{1}{(a+bt)^2} \tag{3}$$

where $\mathrm{EL}_{\mathrm{delayed}}$ is the intensity of the delayed EL, and a and b are constants. The equation appears to be approximately linear in a log–log plot (though deviating from this at early times). The delayed EL contributes a significant fraction of the steady-state EL intensity. For rubrene-based device, this contribution is as high as ≈60%. For other fluorescent dopants (DPA, perylene, and TIPS-pentacene), the emission from the delayed component is 26%–38% of the total EL. It is interesting to note that this process also effectively occurs in TIPS-pentacene. By itself in the solid state it exhibits singlet fission to triplet exciton pair,[21] and $E(\mathrm{S}_1)$ is considered to be close in energy to $2E(\mathrm{T}_1)$. As used here, dispersed in PVK, there is little evidence for effective fission process because the PL lifetime (Figure 1c) indicates efficient radiative emission. In comparison, a very similar device based on an archetypical phosphorescent emitter, PtOEP,[3] was tested. The EL decay of the PtOEP device exhibits no prompt emission but a monoexponential slow emission originating from phosphorescence, with a characteristic decay lifetime of approximately 60 μs.

Next, we investigate how the delayed EL responds to the change of externally injected current. Figure 2b shows the transient-EL profiles for a rubrene device at different current densities. We observe a reduction of the delayed EL component, from 60% to 31%, as the current density increases by two orders of magnitude. This phenomenon can be explained by charge-triplet annihilation at higher current densities,[7] when the balance of injected electrons and holes is not well maintained. It also implies that triplet fusion in the device is very effective even at low current densities. At higher current densities, the possible enhancement of triplet fusion is masked by the detrimental effect of charge quenching. We note that at early times (t < 3 μs), the apparent lifetime of triplet excitons even at low current densities is in the order of a few μs, significantly shorter than the triplet lifetimes identified in rubrene crystals (about 100 μs)[24] and optical TTA-upconverters with a polymer host (up to about 1 ms).[25] However, due to the bimolecular nature of the triplet fusion process, the decay of triplet density (n_T), described by $\mathrm{d}n_\mathrm{T}/\mathrm{d}t = -k_\mathrm{T}n_\mathrm{T} - k_\mathrm{TTA}n^2_\mathrm{T}$, at high population density regime is dominated by the rate of TTA (k_TTA), and is significantly faster than the intrinsic monomolecular decay rate of triplets (k_T) ($k_\mathrm{total} = k_\mathrm{T} + k_\mathrm{TTA}n_\mathrm{T} \approx k_\mathrm{TTA}n_\mathrm{T}$, as $k_\mathrm{TTA}n_\mathrm{T} >> k_\mathrm{T}$). Therefore, the apparent lifetime of the triplet is expected to be significantly shortened when the TTA-UC process is efficient, as the efficient generation of singlets rapidly reduces triplet population. To estimate the monoexcitonic lifetime of triplets, we investigate the EL kinetics of later times (t ≈ 10 μs) when the triplet density is reduced significantly and monomolecular

decay of triplets becomes dominant ($k_T >> k_{TTA}n_T$). We infer a lower bound of 25 µs for the triplet lifetime in the rubrene device.

Besides, increasing current pulse width (from 1 to 500 µs) at a fixed current density (1 mA cm^{-2}) leads to an increase of the delayed EL intensity, from 16% to 51% (Figure 2c). This result agrees with our interpretation that the delayed EL originates from triplet fusion, in which the intensity of delayed fluorescence is related to the population density of triplets.

We measured the magnetic field dependence of EL intensity for the device. The EL increases first when the magnetic field strength reaches 20 mT and reduces monotonically as the field intensity increases further (Figure 2d). This observation is consistent with TTA-induced magneto-EL behavior of OLEDs,[26] further confirming that TTA plays an essential role in the EL of our devices.

Figure 3a shows the emission spectra and photographs of the working LEDs. The DPA device shows efficient deep-blue emission peaked at 440 nm. Perylene, rubrene, and TIPS-pentacene devices exhibit green, yellow, and red EL centered at 520, 570, and 670 nm, respectively. The luminance–voltage characteristics are shown in Figure 3b. Peak luminance of over 7000 cd m^{-2} have been achieved with both rubrene and perylene. Maximum external quantum efficiencies (EQE) of about 6% or above have been obtained for DPA, perylene, and rubrene (Figure 3c and Table S1, Supporting Information). These values exceed the EQE limit (5%) of conventional electrofluorescence (assuming an optical outcoupling factor of 0.2),[6–8] suggesting a significant contribution from triplets toward the total EL. We found that a high emitter doping concentration (20%) results in optimum OLED performance (Figure S2, Supporting Information), consistent with the view that a small intermolecular separation is required for efficient bimolecular TTA process. Increased doping concentration also leads to more pronounced lower-energy spectral features in the EL, as a result of enhanced intermolecular interactions. However, we note that the efficiency roll-off is significant at low current densities, indicating unbalanced charge injection and transport in these unoptimized devices.

To improve charge injection and transport, we developed a solution-processed, inverted multilayer OLED structure (inset of Figure 3e) using ZnO electron-injection layer deposited from solution by atmospheric pressure spatial atomic layer deposition (AP-SALD).[27] Interfacial energy level modification of the ZnO was achieved by a spin-coated polyethylenimine layer.[28] For the emissive layer, we selected rubrene as the emitter (for its superior triplet fusion properties) and a conjugated polymer poly (9,9′-dioctylfluorene)-*co*-benzothiadiazole (F8BT) as the host matrix.[29] We observed that the EL emission was dominated by the emission of rubrene (Figure S3, Supporting Information), confirming the effectiveness of the host–guest energy transfer. We deposited a hole-transport/electron-blocking layer of *N*,*N*′-bis(3-methylphenyl)-*N*,*N*′-diphenylbenzidine (TPD)[30] from solution for the first time. This simply prepared layer effectively reduces exciton quenching by the MoO_x/Au anode. The novel device architecture results in a very low, sub-bandgap turn-on voltage of 1.8 V and a high maximum brightness of 6×10^4 cd m^{-2} (Figure 3e). The maximum EQE obtained from the inverted FuLED is 6.3%, corresponding to a current efficiency of 20.7 cd A^{-1} (Figure 3f), outperforming other solution-processed rubrene OLEDs in the literature. The efficiency roll-off is not apparent across a wide range of current densities (up to 100 mA cm^{-2}), indicating excellent charge balance. We also measured the transient-EL characteristics of the F8BT:rubrene device and compared it with a pristine F8BT device prepared in the same way. A significant difference in the EL kinetics was observed. It showed that the contribution of the delayed EL for the rubrene-doped F8BT was 55% when held at 10 mA cm^{-2}, much higher than the 9% delayed EL contribution observed in the F8BT-only device (Figure 3g). This result suggests that the triplet-fusion process in rubrene-doped F8BT is more efficient than in pure F8BT. In contrast to the standard PVK:rubrene device, the delayed EL contribution in the inverted F8BT:rubrene device is relatively constant, at 50%–60%, across a range of current densities (1–100 mA cm^{-2}). This, together with the insignificant efficiency roll-off, agrees with our previous discussion that the reduced TTA-fusion-related EL component at higher currents is due to unbalanced charge injection and transport, which are minimized in the inverted device architecture.

Our transient-EL and EQE results allow us to evaluate the efficiency of the TTA-UC process in these high-performance FuLEDs. **Figure 4**a illustrates the detailed balance of particle conversion processes in the system. The intrinsic efficiency of the TTA-UC reaction is characterized by $\eta_{TTA\text{-}UC}$ = 2 × number of singlets generated by TTA-UC process/number of triplets entering the TTA upconverter. This can be calculated using experimentally measurable quantities, as:

$$\eta_{TTA\text{-}UC} = \frac{2 \times f_{delayed} \times IQE_{EL} \div PLQE}{f_{excitons} \times f_{triplets}} = \frac{2 \times f_{delayed} \times EQE_{EL}}{f_{excitons} \times f_{triplets} \times f_{outcoupling} \times PLQE} \quad (4)$$

where IQE_{EL} and EQE_{EL} are the internal and external quantum efficiencies of the FuLED, $f_{delayed}$ is the percentage of the delayed EL in the total EL, $f_{excitons}$ is the formation probability of excitons from externally injected charges, $f_{triplets}$ is the fraction of triplet excitons in the initial exciton population formed by charge injection, $f_{outcoupling}$ is the optical outcoupling efficiency of the LED, and PLQE is the photoluminescence quantum yield of the emitter. $f_{excitons}$ is assumed to be 1 for the most conservative estimation. $f_{triplets}$ is assumed to be 0.75 according to spin statistics. $f_{outcoupling}$ is assumed to be 0.2.[6–8]

A more practical quantity we investigate is the TTA-UC quantum yield (or triplet-to-photon quantum yield), $\Phi_{TTA\text{-}UC}$, which calculates the number of TTA-generated photons emitted per triplet exciton entering the upconverter. It is given by the following equation:

$$\Phi_{TTA\text{-}UC} = \frac{f_{delayed} \times IQE_{EL}}{f_{excitons} \times f_{triplets}} = \frac{f_{delayed} \times EQE_{EL}}{f_{excitons} \times f_{triplets} \times f_{outcoupling}} \quad (5)$$

The TTA-upconversion efficiencies and quantum yields of various TTA-UC emitters investigated in this work are

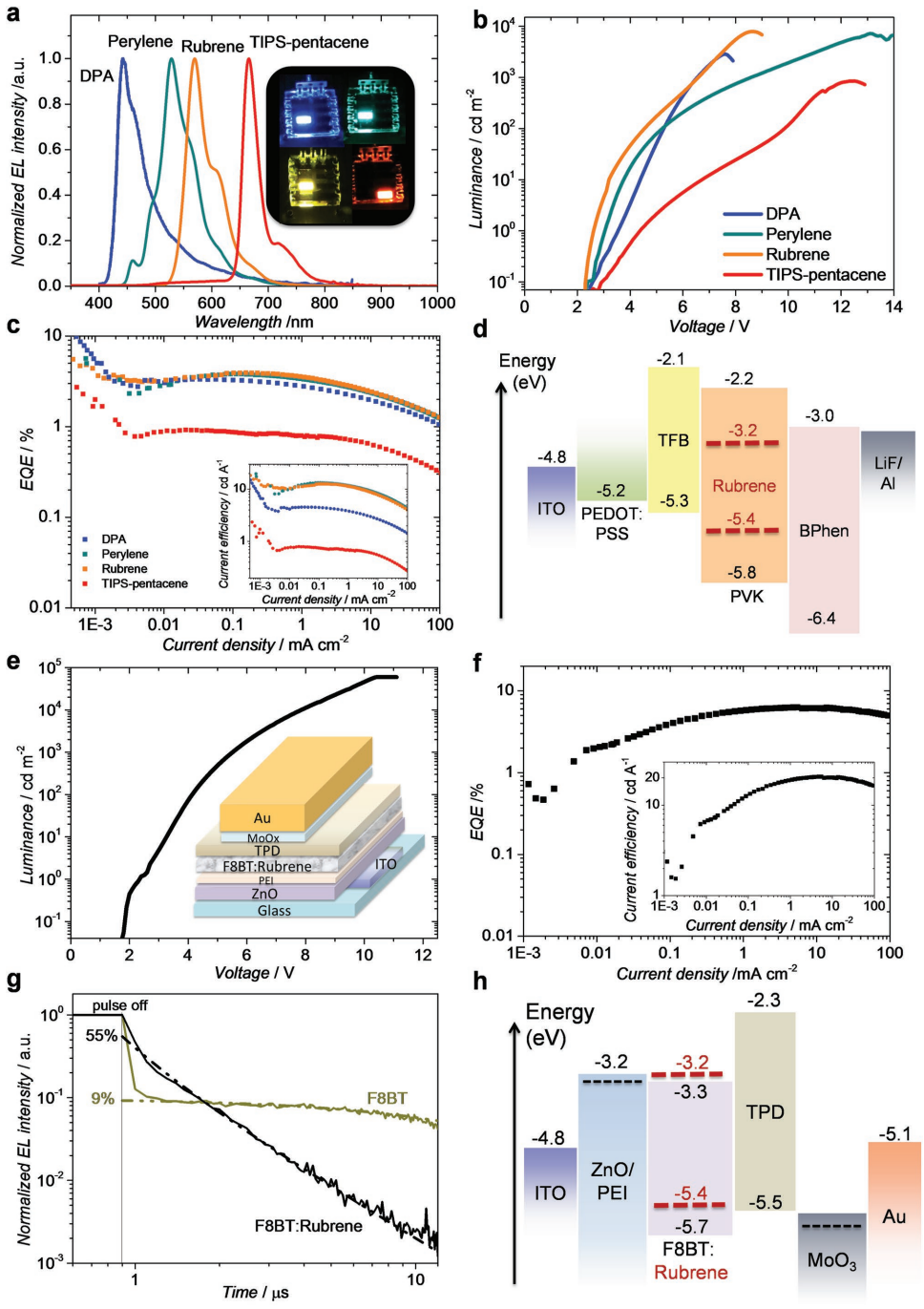

Figure 3. Performance and characterization of FuLEDs. *For standard devices*: a) EL spectra (inset: photographs of working devices). b) Luminance–voltage characteristics. c) EQE versus current density (inset: current efficiency–current density curves). d) Energy level diagram. For inverted device: e) Luminance–voltage curves (inset: device structure). f) EQE versus current density curve (inset: current efficiency versus current density). g) Transient-EL measurements after holding the devices at a current density of 10 mA cm^{-2}. h) Device energy level diagram.

summarized in Figure 4b. The highest $\Phi_{TTA\text{-}UC}$ and $\eta_{TTA\text{-}UC}$ for rubrene are 23% and 70%, respectively (For DPA and perylene, the efficiencies are slightly lower). To the best of our knowledge, these values are higher than that of any solid-state TTA-upconverters reported to date[9–14,19] and are comparable to some of the best TTA-UC efficiencies observed in solution-phase systems.[9–12,18] A summary of the efficiencies of solution systems[17,18,31–33] is shown in Table S2 (Supporting Information). Comparisons of our devices with other solid-state TTA-UC systems[13,14,19,31,34] and other TTA-enhanced OLEDs[7,8,35–37] are presented in Tables S3 and S4 (Supporting Information), respectively. The remarkably high TTA-UC efficiencies in our best devices suggest that only singlets are formed during the TTA process. Besides, it is striking to note that the high

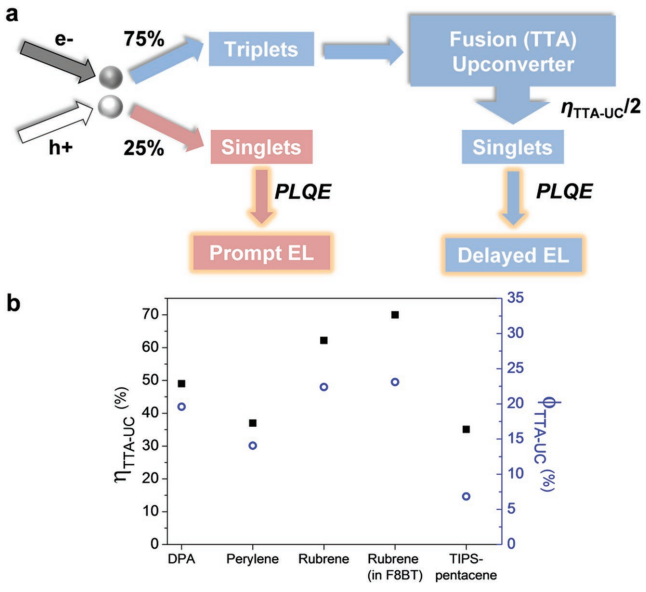

Figure 4. Efficiency evaluation for TTA upconversion in FuLEDs. a) Flow chart of particle conversion processes. b) Triplet-to-photon quantum yield (Φ_{TTA-UC}, ○), and the intrinsic reaction efficiency of TTA-UC (triplet fusion) (η_{TTA-UC}, ■) for different emitters.

TTA-UC efficiencies occur at very low excitation power densities (≈30 mW cm^{-2} for inverted structure and ≈0.001 mW cm^{-2} for standard structure, significantly lower than typical excitation power densities required for optical TTA-upconverters), indicating extremely efficient triplet formation and accumulation in these electroluminescent devices.

Our findings suggest that the processes (such as intersystem crossing and triplet–triplet energy transfer) associated with triplet sensitizer molecules, which are widely used in optically excited TTA-UC systems, are some of the key limiting factors for achieving highly efficient TTA upconversion. The use of a wide-bandgap polymer host provides additional benefit for triplet confinement, ensuring high density and long lifetime of triplets at the same time. For TIPS-pentacene, TTA-UC efficiencies are moderate (η_{TTA-UC} of 35.1% and Φ_{TTA-UC} of 6.8%), likely due to the competing process of singlet fission. However, the observation of the energetically unfavorable triplet fusion process in this material is noteworthy by itself. It is possible that the energy gap between $E(S_1)$ and $2E(T_1)$ in TIPS-pentacene is close to kT, allowing endothermic triplet fusion reaction to effectively take place at room temperature.

Finally, we find that DPA-, rubrene-, and perylene-doped polymer FuLEDs clearly exceed the fluorescence IQE limit of 25% (corresponding to an EQE limit of 5%). The highest IQE value obtained is >30% using the yellow fluorophor, rubrene. The largest percentage contribution of triplet fusion-related electrofluorescence is 60% in rubrene-based FuLEDs. It is by far the highest value observed in TTA-based OLEDs, consistent with the high TTA-UC efficiencies of the emitter molecules. Besides, triplet fusion-related EL contribution of as high as 38% was found in the singlet fission material, TIPS-pentacene.

The very high TTA-UC efficiencies obtained in our FuLEDs and the method we developed to evaluate them provide valuable information for the design of high-efficiency solid-state TTA upconverters for photovoltaics. Our results demonstrate that conventional spin-statistical limits do not apply to these TTA-UC molecules in efficient devices. It also reflects the reciprocity of singlet fission and triplet fusion processes in materials such as TIPS-pentacene. Besides, our efficient, multicolor (deep blue, green, yellow, and red) FuLEDs produced using low-cost solution-processing methods may lead to further technological development toward large-area display and lighting applications.

Supporting Information

Supporting Information is available from the Wiley Online Library or from the author.

Acknowledgements

D.D. and L.Y. contributed equally to this work. D.D. and L.Y. conceived the project with R.H.F., designed the experiments, and performed all data collection and analysis. D.D. and L.Y. carried out the transient-EL experiments with help from J.R., and performed the magnetic-field EL and TCSPC measurements. D.D. and L.Y. developed and characterized the FuLEDs. D.D., K.M., R.M.A., and A.Y.A. developed the ZnO deposition using AP-SALD. J.L.M.-D. provided useful discussions. L.M. assisted with some experiments. D.C. and D.D. cosupervised L.M.'s work. D.D. and L.Y. cowrote the paper, which was revised by R.H.F. D.D. acknowledges the Department of Physics (University of Cambridge) and the KACST–Cambridge University Joint Centre of Excellence for financial support. L.Y. thanks the Singapore Agency for Science, Technology and Research (A*STAR) for a PhD studentship. The authors thank the Engineering and Physical Sciences Research Council (EPSRC) for financial support.

Received: November 6, 2016
Revised: December 6, 2016
Published online: February 1, 2017

[1] C. W. Tang, S. A. Vanslyke, *Appl. Phys. Lett.* **1987**, *51*, 913.
[2] J. H. Burroughes, D. D. C. Bradley, A. R. Brown, R. N. Marks, K. Mackay, R. H. Friend, P. L. Burns, A. B. Holmes, *Nature* **1990**, *347*, 539.
[3] M. A. Baldo, D. F. O'Brien, Y. You, A. Shoustikov, S. Sibley, M. E. Thompson, S. R. Forrest, *Nature* **1998**, *395*, 151.
[4] Y. Ma, H. Zhang, J. Shen, C. Che, *Synth. Met.* **1998**, *94*, 245.
[5] H. Uoyama, K. Goushi, K. Shizu, H. Nomura, C. Adachi, *Nature* **2012**, *492*, 234.
[6] D. Y. Kondakov, *J. Appl. Phys.* **2007**, *102*, 98.
[7] B. H. Wallikewitz, D. Kabra, S. Gélinas, R. H. Friend, *Phys. Rev. B: Condens. Matter Mater. Phys.* **2012**, *85*, 22.
[8] C. J. Chiang, A. Kimyonok, M. K. Etherington, G. C. Griffiths, V. Jankus, F. Turksoy, A. P. Monkman, *Adv. Funct. Mater.* **2013**, *23*, 739.
[9] T. N. Singh-Rachford, F. N. Castellano, *Coord. Chem. Rev.* **2010**, *254*, 2560.
[10] V. Gray, D. Dzebo, M. Abrahamsson, B. Albinsson, K. Moth-Poulsen, *Phys. Chem. Chem. Phys.* **2014**, *16*, 10345.
[11] J. Zhou, Q. Liu, W. Feng, Y. Sun, F. Li, *Chem. Rev.* **2015**, *115*, 395.
[12] T. F. Schulze, T. W. Schmidt, *Energy Environ. Sci.* **2015**, *8*, 103.
[13] P. Mahato, A. Monguzzi, N. Yanai, T. Yamada, N. Kimizuka, *Nat. Mater.* **2015**, *14*, 924.

[14] M. Wu, D. N. Congreve, M. W. B. Wilson, J. Jean, N. Geva, M. Welborn, T. Van Voorhis, V. Bulovi, M. G. Bawendi, M. A. Baldo, *Nat. Photonics* **2015**, *10*, 31.
[15] S. Baluschev, T. Miteva, V. Yakutkin, G. Nelles, A. Yasuda, G. Wegner, *Phys. Rev. Lett.* **2006**, *97*, 7.
[16] C. Zhang, J. Zhao, S. Wu, Z. Wang, W. Wu, J. Ma, S. Guo, L. Huang, *J. Am. Chem. Soc.* **2013**, *135*, 10566.
[17] Y. Y. Cheng, T. Khoury, R. G. C. R. Clady, M. J. Y. Tayebjee, N. J. Ekins-Daukes, M. J. Crossley, T. W. Schmidt, *Phys. Chem. Chem. Phys.* **2010**, *12*, 66.
[18] T. Ogawa, N. Yanai, A. Monguzzi, N. Kimizuka, *Sci. Rep.* **2015**, *5*, 10882.
[19] J.-H. Kim, F. Deng, F. N. Castellano, J. Kim, *Chem. Mater.* **2012**, *24*, 2250.
[20] B. J. Walker, A. J. Musser, D. Beljonne, R. H. Friend, *Nat. Chem.* **2013**, *5*, 1019.
[21] L. Yang, M. Tabachnyk, S. L. Bayliss, M. L. Böhm, K. Broch, N. C. Greenham, R. H. Friend, B. Ehrler, *Nano Lett.* **2015**, *15*, 354.
[22] C.-L. Lee, K. B. Lee, J.-J. Kim, *Appl. Phys. Lett.* **2000**, *77*, 2280.
[23] N. Chandrasekharan, L. A. Kelly, *J. Am. Chem. Soc.* **2001**, *123*, 9898.
[24] A. Ryasnyanskiy, I. Biaggio, *Phys. Rev. B* **2011**, *84*, 193203.
[25] A. Monguzzi, M. Mauri, M. Frigoli, J. Pedrini, R. Simonutti, C. Larpent, G. Vaccaro, M. Sassi, F. Meinardi, *J. Phys. Chem. Lett.* **2016**, *7*, 2779.
[26] C. Gärditz, A. G. Mückl, M. Cölle, *J. Appl. Phys.* **2005**, *98*, 104507.
[27] R. L. Z. Hoye, D. Muñoz-Rojas, D. C. Iza, K. P. Musselman, J. L. MacManus-Driscoll, *Sol. Energy Mater. Sol. Cells* **2013**, *116*, 197.
[28] Y. Zhou, C. Fuentes-Hernandez, J. Shim, J. Meyer, A. J. Giordano, H. Li, P. Winget, T. Papadopoulos, H. Cheun, J. Kim, M. Fenoll, A. Dindar, W. Haske, E. Najafabadi, T. M. Khan, H. Sojoudi, S. Barlow, S. Graham, J.-L. Bredas, S. R. Marder, A. Kahn, B. Kippelen, *Science* **2012**, *336*, 327.
[29] D. Kabra, L. P. Lu, M. H. Song, H. J. Snaith, R. H. Friend, *Adv. Mater.* **2010**, *22*, 3194.
[30] M. Kinoshita, H. Kita, Y. Shirota, *Adv. Funct. Mater.* **2002**, *12*, 780.
[31] A. Monguzzi, R. Tubino, S. Hoseinkhani, M. Campione, F. Meinardi, *Phys. Chem. Chem. Phys.* **2012**, *14*, 4322.
[32] S. Guo, W. Wu, H. Guo, J. Zhao, *J. Org. Chem.* **2012**, *77*, 3933.
[33] R. S. Khnayzer, J. Blumhoff, J. A. Harrington, A. Haefele, F. Deng, F. N. Castellano, *Chem. Commun.* **2012**, *48*, 209.
[34] A. Monguzzi, M. Frigoli, C. Larpent, R. Tubino, F. Meinardi, *Adv. Funct. Mater.* **2012**, *22*, 139.
[35] D. Y. Kondakov, *J. Soc. Inf. Disp.* **2009**, *17*, 137.
[36] D. Y. Kondakov, T. D. Pawlik, T. K. Hatwar, J. P. Spindler, *J. Appl. Phys.* **2009**, *106*, 124510.
[37] J. P. Spindler, W. J. Begley, T. K. Hatwar, D. Y. Kondakov, *SID Symp. Dig. Tech. Pap.* **2009**, *40*, 420.